Investigation of Nanoparticles and Interface Effects on Organometal Halide Perovskite Solar Cells Fabricated by Wet Process

メタデータ	言語: eng
	出版者:
	公開日: 2017-10-05
	キーワード (Ja):
	キーワード (En):
	作成者:
	メールアドレス:
	所属:
URL	http://hdl.handle.net/2297/46582

INVESTIGATION OF NANOPARTICLES AND INTERFACE EFFECTS ON ORGANOMETAL HALIDE PEROVSKITE SOLAR CELLS FABRICATED BY WET PROCESS

A DISSERTATION

SUBMITTED TO THE DIVISION OF MATERIAL SCIENCE

IN PARTIAL FULFILLMENT OF THE REQUIREMENTS FOR THE

DEGREE OF DOCTORATE IN PHILOSOPHY

by

MD. SHAHIDUZZAMAN

REGISTRATION NO.: 1323132008

ADVISOR: DR. TETSUYA TAIMA

GRADUATE SCHOOL OF NATURAL SCIENCE & TECHNOLOGY

KANAZAWA UNIVERSITY

KAKUMA, KANAZAWA, JAPAN

SEPTEMBER, 2016

Abstract

Hybrid organometal halide perovskites such as methylammonium lead iodide ($CH_3NH_3PbI_3$) are attracting considerable attention as energy-efficient light absorber materials for photovoltaic applications owing to their solution processability, tunable bandgap, strong absorption coefficients and cost effectiveness. We, (Dr. Taima research group) developed nano-structured, and interlayer controlled method. This interlayer method, I applied to planar heterojunction (PHJ) perovskite solar cells. My thesis presented two different approaches that are aimed at contributing to the development of PHJ perovskite solar cells.

We prepared $CH_3NH_3PbI_3$ nanoparticles (NPs) for the first time using a simple spin-coating method by incorporating a small amount (1~10 wt %) of an ionic liquid (IL) 1-hexyl-3-methylimidazolium chloride in 25 wt % solution of $CH_3NH_3PbI_3$ in N,N-dimethylformamide (DMF) onto the compact-TiO_x/ITO substrates to control size and shape of NPs. Compact-TiO_x films were prepared by chemical bath deposition (CBD) according to the procedure described by Kuwabara *et al.* (*Organic electronics* 11, **2010**, 1136). The $CH_3NH_3PbI_3$ NP thin films were uniform and free of pin holes, and the excellent morphology was due to the addition of IL. The small-sized $CH_3NH_3PbI_3$ NPs (~350 nm) with superior optical absorption properties have been obtained with 3 wt % of IL in the medium, as compared to the other compositions with wt % of 1, 7 and 10. As a result, a maximum power conversion efficiency (PCE) of 2.81% was obtained with the solar cell using 3 wt % of IL in a solution. The effect of viscosity of varying ILs have also been investigated. Low viscosity of ILs together with completely dissolve in $CH_3NH_3PbI_3$ solution were playing a significant role in controlling the morphology of resulting NPs.

The preliminary results are promising for the fabrication of solar cells based on $CH_3NH_3PbI_3$ NPs using a device configuration of ITO/TiO_x/ $CH_3NH_3PbI_3$ NPs/ spiro-OMeTAD/Ag. We also expect that the results will open a pathway towards a better understanding for the fabrication, modification and enhancement of the performance of solar cells with $CH_3NH_3PbI_3$ NPs. In the present case, we assume a hindering effect followed by impact on charge dissociation, transport, and/or recombination on the device performances due to the residual IL content remained on the $CH_3NH_3PbI_3$ NP films.

And, we fabricated PHJ type perovskite solar cells with enhanced efficiency by introducing fullerene (C_{60}) interlayers with thicknesses of 0, 3, 7 and 10 nm between air-stable amorphous compact TiO_x and $CH_3NH_3PbI_3$ layers. The modified morphology obtained by inclusion of C_{60} improved the surface energy properties of the cells in terms of enhanced photocurrent. Atomic force microscopy verified the correlation between the surface energy and phase morphology of the PHJ solar cells. The introduction of a C_{60} interlayer between $CH_3NH_3PbI_3$ and TiO_x layers increased the content of photogenerated charge carrier sites, as well as lowering the accumulation and trapping of photogenerated charges at the TiO_x interface. The optimum thickness of C_{60} interlayer was 7 nm, for which a maximum PCE of 9.51% was obtained.

Keywords: Nanoparticles; Ionic liquid; Spin-coating method; Organometal halide perovskite; $CH_3NH_3PbI_3$; Interlayer; Fullerene (C_{60}).

Results and discussion

We introduced varying wt % of IL (chemical structure: Fig. 1a) as a morphology controlling additive with $CH_3NH_3PbI_3$ in the DMF solution. We obtained a clear yellow-orange colored homogeneous solution having no aggregate or NPs (Fig. 1b).

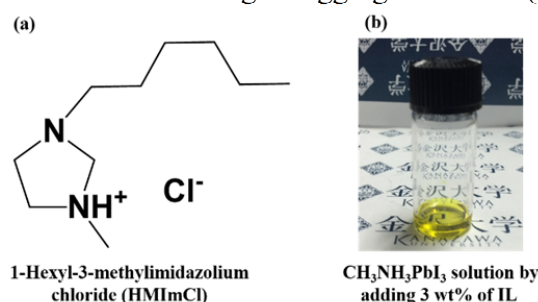**Figure 1.1.** (a) Chemical structure of 1-hexyl-3-methylimidazolium chloride (HMImCl), (b) Homogeneous mixture solution of $CH_3NH_3PbI_3$ and IL.

$CH_3NH_3PbI_3$ NPs having spherical morphology, was formed as shown in Fig. 1.2 (a, b and c), in the presence of 1, 3 and 7 wt % IL with respective diameters of 540, 350 and 600 nm. In contrary, the addition of high concentration of 10 wt % IL has resulted in irregular aggregation of $CH_3NH_3PbI_3$ blocks as shown in Fig. 1.2d. We observed unchanged shapes but changed morphology of NPs with varying wt % of IL to the solution. The observation was similar to a previous report by Duan *et al.*[1] which confirms that the sizes and morphologies of the crystals depended on the concentration of the ionic liquid.

The observation was further confirmed by the AFM analysis. The AFM image (Fig. 1.3e-f), showed the aggregated morphology of NPs with non-uniform distribution for 7 and 10 wt % IL in solution, while the morphology was well developed for 1 and 3 wt % IL in solution as shown in Fig. 1.3c-d, respectively. The root-mean-square (RMS) roughness of the $CH_3NH_3PbI_3$ films were respectively 21.19, 17.83, 71.25 and 121.29 nm at 1, 3, 7 and 10 wt % of IL. The RMS roughness was smoother with 3 wt % IL in solution as compared to the other compositions. Air stable amorphous compact-TiO_x layer having smooth morphology of 30 nm thickness was achieved in one-time operation as shown in the AFM analysis (Fig. 1.3a). The RMS roughness value of the resulting film was 4.13 nm.
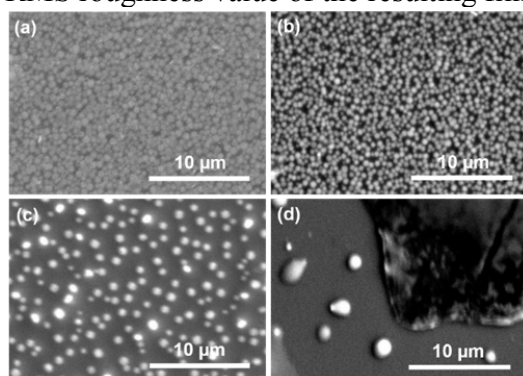

Figure 1.2. The SEM images of the $CH_3NH_3PbI_3$ NPs prepared in the presence of varying concentration of IL: (a) 1 wt %, (b) 3 wt %, (c) 7 wt %, and (d) 10 wt %.

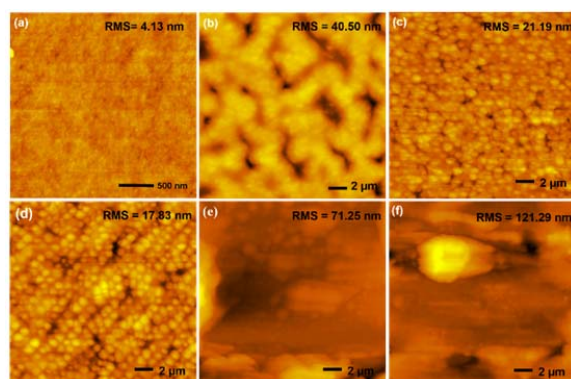**Figure 1.3.** The AFM images of (a) TiO_x film; (b) As-deposited $CH_3NH_3PbI_3$ small clusters prepared at RT and $CH_3NH_3PbI_3$ NPs with varying concentration of IL: (c) 1 wt %, (d) 3 wt %, (e) 7 wt %, and (f) 10 wt %.

The UV-Vis spectra of $CH_3NH_3PbI_3$ films with varying wt % of IL cast on glass/ITO/ compact-TiO_x substrates are shown in Fig. 1.4. The absorption spectrum of DMF was discovered at around 263 nm (not shown in Figure), while it was at 340 nm for only IL. The optical properties of $CH_3NH_3PbI_3$ NPs depend on the size and the shape of the particles. The absorption peaks were observed at around 493, 550, 520 and 525 nm in the system with 1, 3, 7 and 10 wt % IL, respectively, which corresponded to NPs, in accordance with the observation from Ayi, *et al.*[2] The sharp absorption peaks for the spherical NPs also indicated a fairly uniform shape and size of NPs.
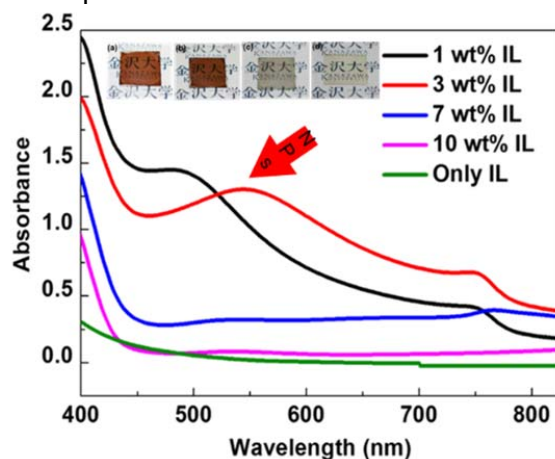

Figure 1.4. The UV-Vis spectra of the $CH_3NH_3PbI_3$ films processed with varying wt % of IL as well as only IL. Inset photographs show $CH_3NH_3PbI_3$ films prepared with varying concentration of IL: (a) 1 wt %, (b) 3 wt %, (c) 7 wt %, and (d) 10 wt %.

It was clear that the concentration of IL played a vital role on the sizes, shapes and morphologies of the $CH_3NH_3PbI_3$ NPs. A uniform $CH_3NH_3PbI_3$ NPs with well-defined morphologies have been obtained in the presence of a small amount of IL as additive (Figure 1.2a-d). When the amount of the IL increased to 7 wt %, we obtained spherical $CH_3NH_3PbI_3$ NPs (Fig. 3.2c) having approximately 600 nm diameter. In contrast, 3 wt % of

IL was the optimum condition leading to the formation of uniform $CH_3NH_3PbI_3$ NPs with a well-controlled spherical NPs with approximate diameter of 350 nm (Fig. 3.2b). However, when the amount of IL was increased to 10 wt %, we obtained amorphous $CH_3NH_3PbI_3$ blocks formed by irregular aggregation of small particles (Fig. 1.2d). We attributed it to the viscosity of the IL-DMF medium. A similar observation for IL-water medium was reported by Wu *et al.*[3] and the exponential expression used to express such characteristics were modified to fit into our system:

$$\eta = \eta_{IL} \cdot \exp\left[{}^{-x_c}/_a\right] \qquad (1)$$

In Eq (1), x_c is the mole fraction of DMF, a is a characteristic constant of the mixture, and η_{IL} is the viscosity of the pure IL. The empirical equation point out that the viscosity of IL-DMF mixtures is increased exponentially when the mole fraction of DMF (x_c) is decreased. When the amount of IL is increased, the viscosity of the system increases and the diffusion of the resulting complexes hindered. The resulting uniform thin film with good morphology was due to the presence of the IL.

Figure 1.5a showed the device configuration of solar cells based on $CH_3NH_3PbI_3$ NPs. The current density versus voltage (*J-V*) characteristics of $CH_3NH_3PbI_3$ NPs based solar cells as obtained by using the varying concentration of IL (1, 3 and 7 wt %) and were measured at AM 1.5G illuminations are shown in Figure 1.5b. The photovoltaic devices prepared with 1 wt % IL-doped $CH_3NH_3PbI_3$ NPs showed a short-circuit current density (J_{sc}) of 4.84 mA/cm^2. An increase in the J_{sc} value to 5.74 mA/cm^2 was observed for the photovoltaic device prepared using 3 wt % IL-doped $CH_3NH_3PbI_3$ NPs, while the J_{sc} value is decreased to 2.56 mA/cm^2 for 7 wt % doping of IL. The power conversion efficiency (PCE) is also followed the similar trend of the J_{sc} values, showing a higher PCE of 2.81% for the photovoltaic device of 3 wt % IL-doped $CH_3NH_3PbI_3$ NPs. All the parameters measured to study the performances of solar cells are summarized in Table 1. Optimization of the concentration with the 3 wt % of IL, we achieved $CH_3NH_3PbI_3$ NPs having more uniform shape, size, morphology which showed maximum PCE. Currently, we assume a hindering effect followed by the impact on charge dissociation, transport, and/or recombination on the device performances due to the residual IL content within the $CH_3NH_3PbI_3$ NPs. Hence, performance improvement experiments are underway to ensure the complete removal of IL-contents from the $CH_3NH_3PbI_3$ NPs films.

Table 1. Summary of cell performances of ITO/Compact-TiO_x/$CH_3NH_3PbI_3$ NPs/Spiro-OMeTAD/Ag

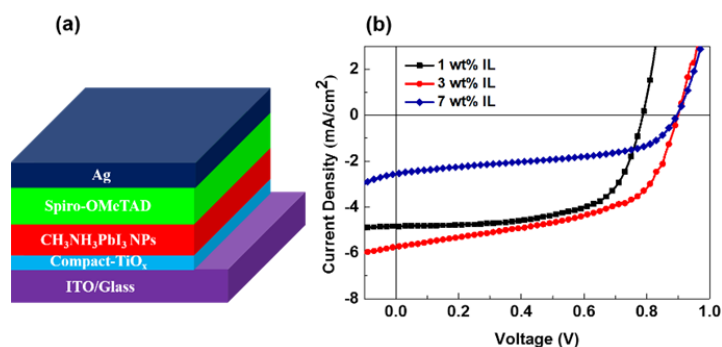| Wt % of IL	J_{sc}/mAcm^{-2}	V_{oc}/V	FF	PCE %
1	4.84	0.78	0.64	2.44
3	5.74	0.89	0.55	2.81
7	2.56	0.89	0.50	1.14

Figure 1.5. (a) Device configuration of solar cells based on $CH_3NH_3PbI_3$ NPs; (b) The *J-V* characteristics obtained for the solar cells based on $CH_3NH_3PbI_3$ NPs.

And, in this work, we modify the surface characteristics of air-stable amorphous TiO_x layers by inserting fullerene (C_{60}) as an interlayer in PHJ solar cells and investigate the effect of the thickness of the C_{60} interlayer on the morphology and power conversion efficiency (PCE) of the resulting devices. Varying the thickness of the C_{60} interlayer between 0 and 10 nm allows us to control the surface energy of the cells over a wide range of values. A correlation between the surface energy and PCE in PHJ solar cells is established, offering the possibility to enhance device performance. PCE is enhanced by the increased photocurrent that is obtained by tuning surface energy through optimization of morphology.

The AFM image in Fig. 1.6(a) reveals that a uniformly distributed, compact-TiO_x amorphous layer with a thickness of 60 nm was obtained from two deposition cycles. The root-mean-square (RMS) roughness of this film was 4.21 nm. Fig. 1.6(b), (c) and (d) show the uniformly distributed morphologies of the C_{60} interlayers with thicknesses of 3, 7 and 10 nm, respectively, which have respective RMS roughness values of 4.12, 3.31 and 8.28 nm. The RMS roughness was smoother with 7 nm C_{60} film as compare to the other film thickness. The better morphology of 7 nm C_{60} interlayer can be collected electrons more efficiently at the $CH_3NH_3PbI_3$/compact-TiO_x interface, thus degrading the interfacial barrier. As compared to other conditions, the morphology becomes more rough (Figure 1.6 b and d), which is expected to reduce the interfacial area. The resultant reduction of charge generation then will degrade the J_{SC} (and hence also the PCE). The variation of the device performance with respect to the surface energy observed in Figure 1.6 and 1.7 can be explained in terms of morphology. The films without C_{60} showed incomplete surface coverage and were composed of non-uniform large ribbon-like crystals (Fig. 1.6(e)).
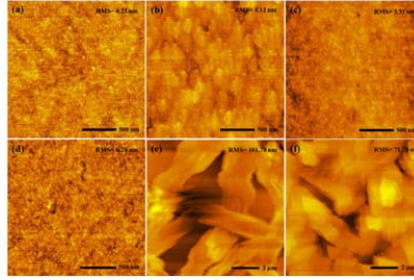
Figure 1.6. AFM images of (a) a TiO_x film; C_{60} layers with a thickness of (b) 3, (c) 7, and (d) 10 nm; (e) $TiO_x/CH_3NH_3PbI_3$ film and (f) TiO_x/C_{60} (7 nm)/$CH_3NH_3PbI_3$ film

RMS roughness values of the $CH_3NH_3PbI_3$ films with and without a 7-nm-thick C_{60} layer were 71.78 and 101.78 nm, respectively, so the 7-nm-thick C_{60} interlayer decreased the roughness of the overlying $CH_3NH_3PbI_3$ film. To produce highly efficient PHJ perovskite solar cells, it has been shown that uniform morphology and high crystallinity are very important.[4, 5] In this respect, both the morphology and crystallinity of perovskite solar cells have been improved by inclusion of a C_{60} interlayer. The enhanced crystallization facilitates the more charge transfer efficiency between interlayer and the $CH_3NH_3PbI_3$.

Figure 1.7 (a), (b) and (d) show J_{sc}, FF and PCE of the cells, respectively, as a function of TiO_x surface energy in the range from 43 to 51.5 mJ m^{-2}. J_{sc}, FF and PCE all exhibited the same overall trend with respect to surface energy, with maximum values at an intermediate surface energy. The highest PCE (9.51%), J_{sc} (15.17 mA/cm^2) and FF (0.69) were observed for the device with a surface energy of 51.5 mJ m^{-2} containing a 7-nm-thick C_{60} interlayer. The optimized morphology obtained by surface-energy modification enhanced the photocurrent of the corresponding solar cell. In contrast, the open circuit voltage (V_{oc}) did not show any significant changes with respect to the surface energy, as shown in Figure 5.5b. AFM analysis verified the correlation between the surface energy and phase morphology of the PHJ solar cells.
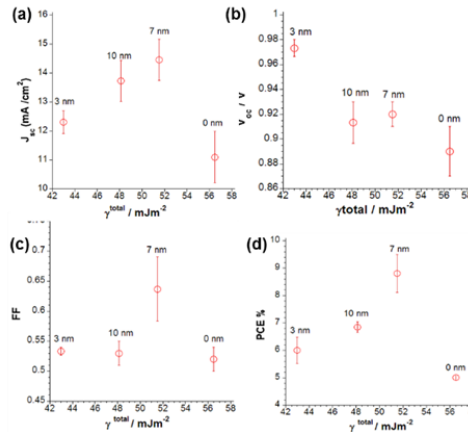

**Figure 1.7.** Characteristics of $CH_3NH_3PbI_3$ solar cells as a function of the surface energy of the C_{60} layer: (a) short-circuit current density, J_{sc}, (b) open-circuit voltage, V_{oc}, (c) fill factor, FF, and (d) power conversion efficiency, PCE. Error bars show plus-or-minus one standard deviation from the mean.

Figure 1.8(a) further compares the device characteristics of the PHJ $CH_3NH_3PbI_3$ solar cells by showing *J-V* curves measured for cells with and without a C_{60} interlayer. A solar cell with similar architecture fabricated using PCBM as the interlayer instead of C_{60} was used as a reference. The device without a C_{60} interlayer exhibited a J_{sc} of 11.98 mA/cm^2, V_{oc} of 0.91 V, FF of 0.49, and PCE of 5.12%. Such poor device performance was caused by a contact barrier that prevented efficient electron injection at the interface between $CH_3NH_3PbI_3$ and TiO_x, which led to a large leakage current and the recombination of charge carriers. Conversely, incorporation of a 7-nm-thick C_{60} interlayer caused J_{sc} to increase to 15.17 mA/cm^2, while it was 13.47 mA/cm^2 for the device with a 10-nm-thick PCBM interlayer. The FF was enhanced from 0.49 to 0.69 and 0.55 upon the inclusion of 7-nm-thick C_{60} and 10-nm-thick PCBM layers, respectively. The enhancement of J_{sc} and FF induced by the 7-nm-thick C_{60} interlayer was attributed to the lowering of the injection barrier at the interface between $CH_3NH_3PbI_3$ and compact TiO_x, which decreased the series resistance from 25.75 to 7.39 Ωcm^2. This result indicates that the incorporation of a C_{60} interlayer on the TiO_x/ITO glass substrate enhanced charge carrier extraction from the perovskite layer to the ITO electrode, which led to the improvement of J_{sc} and PCE of the resulting films. PCE increased considerably from 5.12% to 9.51% upon the insertion of a 7-nm-thick C_{60} interlayer between the $CH_3NH_3PbI_3$ and TiO_x layers.

Incident photon-to-current conversion efficiency (IPCE) curves of devices with and without interlayers are presented in Fig. 1.8(b). The enhanced PCEs of the devices with a C_{60} or PCBM layer are consistent with the higher IPCE values of these devices than that of the cell without an interlayer. The photocurrents determined from the IPCE data were 11.02, 13.12 and 15.17 mA/cm^2 for cells without an interlayer, and with an interlayer of PCBM (10 nm) and C_{60} (7 nm), respectively. The PHJ $CH_3NH_3PbI_3$ solar cells exhibited a spectral response that extended from the visible to the near-infrared region with a broad, flat peak intensity of absorption around 60%–70% at approximately 380–750 nm. The higher IPCE
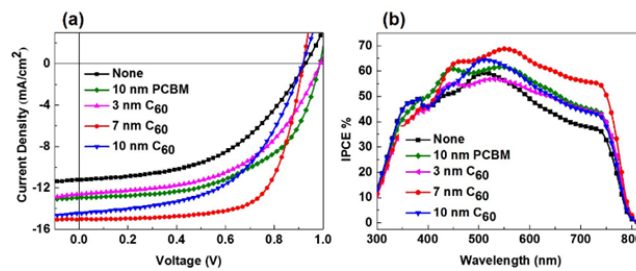
value of the

Figure 1.8. (a) Current density–voltage (*J-V*) characteristics and (b) incident photon-to-current conversion efficiency (IPCE) spectra of devices without and with C_{60} interlayers of different thicknesses.

device with a 7-nm-thick C_{60} layer in the visible-to-near-infrared wavelength region than those of the other devices suggests that the 7-nm-thick C_{60} interlayer collect electrons more

efficiently at the $CH_3NH_3PbI_3/TiO_x$ interface because it successfully lowers the interfacial energy barrier.

Table 2. Performance of cells with the structure $ITO/compact\text{-}TiO_x/C_{60}$ or $CH_3NH_3PbI_3/Spiro\text{-}OMeTAD/Ag$.

Interlayer	J_{sc} (mA/cm^2)	V_{oc} (V)	FF (%)	PCE (%)	Rs ($\Omega.cm^2$)
None	11.98	0.91	0.49	5.12	25.75
10 nm of PCBM	13.47	0.98	0.55	7.04	10.32
3 nm of C_{60}	12.70	0.98	0.52	6.49	18.49
7 nm of C_{60}	15.17	0.93	0.69	9.51	7.39
10 nm of C_{60}	14.44	0.91	0.53	7.04	15.03

The effect of incorporation of a C_{60} interlayer on the performance enhancement of PHJ perovskite solar cells was clarified by including C_{60} interlayers of different thickness. The parameters of these solar cells are summarized in Table 2. The results from these measurements strongly supported our concept that manipulating the surface energy of the C_{60} interlayer can enhance device performance. The above discussion indicates a clear relationship between surface energy, perovskite film morphology and PCE.

Conclusions

We succeeded to prepare $CH_3NH_3PbI_3$ NPs with better morphology by introducing an ILs of varying wt % by using a simple spin-coating method. The results showed that the size and shape of NPs can be controlled or modified by using varying wt % of IL as additive in the DMF solvent medium. The small-sized $CH_3NH_3PbI_3$ NPs (~350 nm) with superior optical absorption properties have been obtained with 3 wt % of IL in the medium, as compared to the other compositions with wt % of 1, 7 and 10. As a result, a maximum PCE of 2.81% was obtained with the solar cell using 3wt % of IL in a solution.

We tuned the surface energy of TiO_x films by introducing C_{60} interlayers of varying thickness into PHJ perovskite solar cells to enhance their PCE. The surface energy of the C_{60} interlayer strongly affected the resulting device performance. The highest PCE was observed for the device fabricated with a 7-nm-thick C_{60} interlayer, which had a surface energy of 51.5 mJ m^{-2}. The C_{60} interlayer between the perovskite and TiO_x layers increased the content of photogenerated charge carrier sites and lowered the accumulation and trapping of photogenerated charges at the TiO_x interface. These effects increased J_{sc}, FF and PCE of the cells containing a C_{60} interlayer compared with those of solar cells without an interlayer. The maximum PCE of 9.51% for the device with a 7-nm-thick C_{60} interlayer can be attributed to its low series resistance caused by better energy level alignment with the contacts, which lowered the interfacial barrier.

References

1. X. Duan, J. Lian, J. Ma, T. Kim and W. Zheng, *Cryst. Growth Des.*, 2010, **10**, 4449-4455.
2. A. A. Ayi, C. A. Anyama and S. S. Etuk, *J. Appl. Chem.*, 2014, **2**, 26–32.
3. L. Wu, J. Lian, G. Sun, X. Kong and W. Zheng, *Eur. J. Inorg. Chem.*, 2009, **2009**, 2897-2900.
4. M. Liu, M. B. Johnston and H. J. Snaith, *Nature*, 2013, **501**, 395-398.
5. N. J. Jeon, J. H. Noh, Y. C. Kim, W. S. Yang, S. Ryu and S. I. Seok, *Nat. Mater.*, 2014, **13**, 897-903.

学位論文審査報告書（甲）

１．学位論文題目（外国語の場合は和訳を付けること。）

Investigation of Nanoparticles and Interface Effects on Organometal Halide Perovskite Solar Cells Fabricated by Wet Process

塗布法で作製されたペロブスカイト太陽電池でのナノ粒子効果および界面効果の検討

２．論文提出者　（1）所　　属　物質科学　専攻

　　　　　　　　（2）氏　　名　Md . Shahiduzzaman
　　　　　　　　　　　（ふり）（がな）　モハマド　シャヒドゥザマン

３．審査結果の要旨（600〜650 字）

　　本審査員会は、提出学位論文に対する個別審査を行った後、平成 28 年 7 月 13 日の予備審査と平成 28 年 8 月 2 日の口頭発表の結果を踏まえ、以下のように判定した。ペロブスカイト太陽電池は、有機・無機ハイブリットの太陽電池であり塗布による低コスト化が可能として注目を集めており、研究開発が活発に行われている。高性能化には、ペロブスカイト膜のナノ構造の制御と金属酸化物や金属電極とのキャリア輸送特性の向上が重要となっている。本論文は、ペロブスカイト膜の塗布製膜において、塗布溶液にイオン液体を添加（1 wt%）することで、粒径 100 nm 程度のナノ粒子化膜を形成できることを見出し、ナノ構造制御に成功した。また、イオン液体の濃度依存性や粘度依存性を評価することでナノ粒子の形成メカニズムの同定を行った。さらに、電荷捕集層の酸化チタン膜とペロブスカイト膜に蒸着により極薄のフラーレン膜を挿入することで、挿入なしの約 2 倍に当たる 9.5%の変換効率の発現に成功した。以上の結果は、ペロブスカイト太陽電池の実用化に関する新技術の実現とそのメカニズム解明に寄与するものであり、委員会は本論文が博士（学術）論文に値すると判定した。

４．審査結果　　（1）判　　定（いずれかに◯印）　　◯合　格　・　不合格
　　　　　　　　（2）授与学位　　博　士（学術）